



PCCP

Insulation of Coumarin Derivative with [1]Rotaxane to Control Solvation-induced Effects in Excited-state Dynamics for Enhanced Luminescence

Journal:	<i>Physical Chemistry Chemical Physics</i>
Manuscript ID	CP-COM-05-2022-002221
Article Type:	Communication
Date Submitted by the Author:	16-May-2022
Complete List of Authors:	Russell, Go; The University of Tokyo Graduate School of Arts and Sciences College of Arts and Sciences, Department of Basic Science Masai, Hiroshi; The University of Tokyo Graduate School of Arts and Sciences College of Arts and Sciences, Department of Basic Science, Graduate School of Art and Sciences Terao, Jun; The University of Tokyo Graduate School of Arts and Sciences College of Arts and Sciences, Department of Basic Science

SCHOLARONE™
Manuscripts

PAPER

Insulation of Coumarin Derivative with [1]Rotaxane to Control Solvation-induced Effects in Excited-state Dynamics for Enhanced Luminescence

Received 00th January 20xx,
Accepted 00th January 20xx

Go M. Russell,^a Hiroshi Masai,^{ab} and Jun Terao^{*a}

DOI: 10.1039/x0xx00000x

A coumarin derivative bearing a [1]rotaxane structure with permethylated β -cyclodextrins suppressed unwanted solvation-induced effects and increased luminescent quantum yields in medium- and high-polarity solvents. The non-radiative decay was suppressed by the twist in the π -conjugated system and the radiative decay was enhanced by the suppression of the polarity-induced structural changes.

1. Introduction

Improving luminescent quantum yields in light-emitting devices and luminescent sensors is of major interest for enhancing material performance.¹ Diverse approaches such as tuning the molecular structures and orbitals of the luminescent chromophores have been developed for the purpose.² Recently, supramolecules such as host-guest capsules, micelles, vesicles, and matrices for controlling the environments around chromophores have gained importance for enhancing quantum yields.³ In particular, insulation of the chromophores from the environment using cyclic molecules, such as pseudorotaxanes and rotaxanes, has attracted considerable attention owing to the simple and effective isolation of the luminescent core from the external environment using stoichiometric cyclic components. For example, the optical properties of π -conjugated molecules typically deteriorate in the solid state owing to strong π - π intermolecular interactions with adjacent molecules. The introduction of cyclic molecules into this system successfully prohibits these unwanted interactions, thus, improving the luminescent properties of the chromophores.⁴

Studies on cyclic insulation to improve luminescent quantum yields have mainly focused on controlling strong interactions, such as π - π interactions, hydrogen bonding, and donor-acceptor interactions.⁵ However, the insulation effects on weak interactions and the dynamics of chromophores with solvents i.e., solvation and solvent-induced dynamics in excited states have not been thoroughly investigated. Although each solvent molecule has weak interactions with the chromophore, the overall solvation effect strongly influences luminescent quantum yields; generally, yields decrease with high solvent

polarity, especially for polar chromophores.⁶ Active control of the solvent environment of chromophores using cyclic molecules would afford further development of luminescent material performance (Fig. 1a).

To achieve effective solvation control, the molecular design must have (i) a high surface coverage for the chromophore to prevent interactions with the small solvent molecules, and (ii) a stable association between the chromophores and cyclic molecules in solvents of various polarities. However, typical rotaxanes and pseudorotaxanes rarely satisfy both conditions because rotaxanes induce dynamic motions of macrocycles

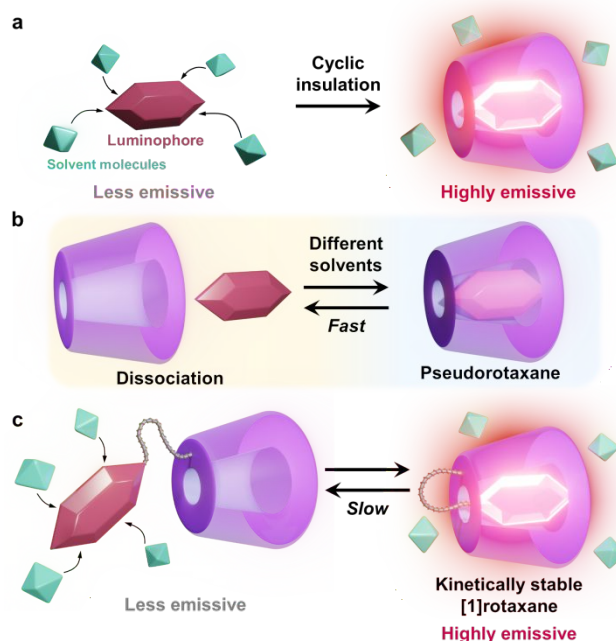


Fig. 1. (a) Schematic representation of cyclic insulation for inhibiting solvation-induced loss of luminescence. (b) The dynamics of pseudorotaxane dissociation upon changing solvents. (c) The concept of a highly emissive luminophore bearing a kinetically stable [1]rotaxane structure (This work).

^a Department of Basic Science, Graduate School of Arts and Sciences, The University of Tokyo, 3-8-1, Komaba, Meguro-ku, Tokyo, 153-8902, Japan

^b PRESTO, Japan Science and Technology Agency, 4-1-8 Honcho, Kawaguchi, Saitama, 332-0012, Japan

Electronic Supplementary Information (ESI) available: [details of any supplementary information available should be included here]. See DOI: 10.1039/x0xx00000x

along the axles, i.e., shuttling, to partially expose the chromophores,⁷ and pseudorotaxanes easily dissociate the supramolecular complexes by changing the solvent polarity (Fig. 1b).⁸ Some rotaxanes strictly fix the cyclic molecules on the chromophores by tightly introducing bulky stoppers near the chromophores to prevent shuttling motions.⁹ Here, to meet both the conditions (i) and (ii), we employed linked rotaxane structures, in which the cyclic molecules are covalently connected to luminescent chromophores as axle components (Fig. 1c).¹⁰ We clarified that the covalent linkages in [1]rotaxanes prevent the dissociation and shuttling of the macrocycles owing to high steric hindrance.¹¹ This structural distinction of linked rotaxanes enables solvation inhibition with high efficiency and provides stable associations in a variety of solvents, affording systematic investigation of the solvation effects on the insulated chromophores.

Various types of insulation effects were demonstrated in our previous studies on insulated structures having linked rotaxanes using permethylated α -cyclodextrins (PM α -CDs).¹² The rotaxane structure improved the luminescent quantum yields by inhibiting molecular interactions in the solid state^{12c} and thermal fluctuations in the solution state.^{12d} However, the effects of solvent insulation on the luminescent quantum yield remain unclear. Recently, we succeeded in exploiting a [1]rotaxane structure using PM α -CDs and a donor-bridge-acceptor (D-B-A) moiety to evaluate the solvation effects of the D-B-A system by comparing the insulated and uninsulated structures.^{12e} The study clearly indicated that insulation with PM α -CD prohibited the interaction of solvent molecules with the conjugated structures. In this study, we applied an insulation strategy for solvation using a linked rotaxane structure to improve the luminescent quantum yields of a fluorescent moiety. Coumarin, a typical fluorescent moiety for laser dyes and probes,¹³ was introduced into a [1]rotaxane structure insulated by a PM α -CD. The optical properties of the insulated coumarin were investigated to determine the solvation-induced kinetic effects of insulation for increasing fluorescent quantum yields.

2. Results and discussion

The [1]rotaxane structure was prepared according to a previously reported strategy (Fig. 2a).¹² A coumarin derivative bearing PM α -CD (**2**) was prepared via deprotection of the trimethylsilyl group of **1**, followed by a Sonogashira coupling reaction between the ethynyl benzene moiety and 7-iodo-4-methylcoumarin. Reduction of the nitro group of **2** to an amino group afforded an uninsulated coumarin, *uns*-**CM**. *uns*-**CM** was converted to a [1]rotaxane structure (*ins*-**CM**) through hydrophobic interactions, which provided high affinity between the diarylacetylene moiety on the coumarin derivative and the PM α -CD. The conversion proceeded quantitatively in MeOH/H₂O (1/1) via a flipping motion i.e., a 360° rotation of the glucopyranose unit of PM α -CD.¹⁴ The full conversion of *uns*-**CM** required a long reaction time (overnight) at room temperature because of the relatively large steric barrier for transformation.¹¹ The insulation structure of *ins*-**CM** was

confirmed by NMR analyses (Fig. 2b). In the ¹H NMR spectra, the aromatic proton signals in *ins*-**CM** shifted downfield compared with those of *uns*-**CM**, because of the characteristic deshielding effect of PM α -CD.¹⁵ Moreover, in the ROESY NMR spectrum of *ins*-**CM**, a strong nuclear Overhauser effect (NOE) was observed between the aromatic protons of the coumarin and the inner protons of PM α -CD (Fig. 2c). In DOSY NMR spectrum of *ins*-**CM**, a single band at logD = -9.37 was observed, which is a similar value to that of *uns*-**CM** (logD = -9.40). The DOSY NMR experiments indicated that the transformation from *uns*-**CM** to *ins*-**CM** was an intramolecular process without any assembly among multiple components of *uns*-**CM**. Hence, the insulated coumarin *ins*-**CM** and its uninsulated counterpart *uns*-**CM** were successfully synthesized as a pair of supramolecular stereoisomers, where the difference in the properties between *ins*-**CM** and *uns*-**CM** arose from the [1]rotaxane supramolecular structure.

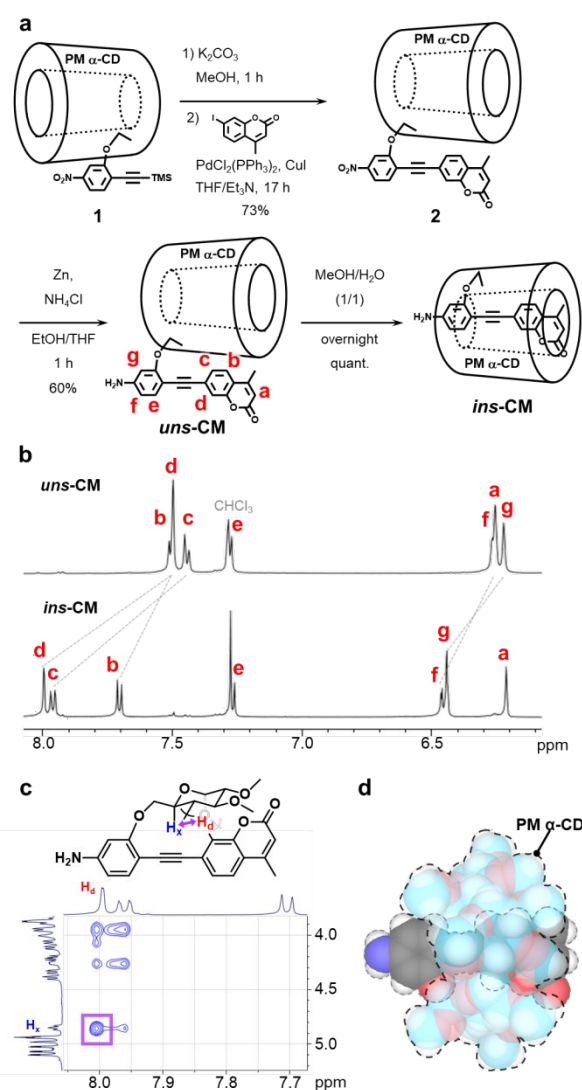


Fig. 2. (a) Synthetic route for *uns*-**CM** and *ins*-**CM**. (b) ¹H NMR spectra of *uns*-**CM** and *ins*-**CM** (500 MHz, CDCl₃, room temperature). (c) Partial ¹H-¹H ROESY NMR spectrum of *ins*-**CM**. (d) Density functional theory-optimized structure of *ins*-**CM** (B3LYP/6-31G(d, p)). Carbon atoms in PM α -CD are shown in cyan and in coumarin in black, oxygen in red, nitrogen in blue, and hydrogen in white.

The computationally optimized structure of *ins-CM* determined by density functional theory (DFT) calculations showed that the coumarin moiety was highly insulated by PM α -CD (Fig. 2d). According to the model, the coumarin core was mostly wrapped with methylated glucopyranose units of PM α -CD. Moreover, the insulated structure of *ins-CM* possessed a high activation barrier for dissociation of the macrocycle owing to the covalent linkage between the axle and cyclic components. The high activation barrier contributed to the stability of the [1]rotaxane structure in various solvents; the insulated molecule *ins-CM* remained intact at room temperature for more than 12 h even in the low-polarity solvent, acetonitrile (MeCN) as shown in Fig. S1. These results demonstrate that the supramolecular structure of *ins-CM* having a high coverage ratio of the dye was kinetically stable even in solvents unfavorable to the insulated structure thermodynamically. Thus, the linked rotaxane structure is ideal for systematic evaluation of solvation-induced effects.

The absorption and emission properties of *ins-CM* and *uns-CM* in MeCN were measured to evaluate the effects of insulation on the optical properties of the luminophore. In addition, the electronic properties of a coumarin derivative bearing a methoxy group instead of PM α -CD in *ins-CM* were obtained by DFT calculations to examine the nature of intramolecular charge transfer (ICT) in the excited state (Fig. S10). Insulated coumarin and uninsulated coumarin had maximum absorption wavelengths at 364 nm and 373 nm, respectively. The hypsochromic shift due to insulation was attributed to the shorter effective conjugation length of *ins-CM* compared with *uns-CM*, which was induced by encapsulation with PM α -CD.¹⁰ Similarly, the maximum emission wavelength was blue-shifted by insulation (*ins-CM*: 537 nm vs. *uns-CM*: 547 nm). It is noteworthy that the quantum yield of *ins-CM* (12.7%) in MeCN was six times higher than that of its uninsulated counterpart *uns-CM* (2.0%) (Fig. 3a). Similarly, in acetone, *ins-CM* displayed a high quantum yield of 33.8%, which was superior to that of *uns-CM* (5.3%). Therefore, insulation of the coumarin derivative improved the fluorescent quantum yield.

The effects of insulation on the coumarin fluorophore under solvation conditions were systematically investigated by measuring the absorption and emission properties in solvents of various polarities (Fig. S2, Table S1). As discussed above, linked rotaxanes possess kinetic stability of the threaded structure in solvents of various polarities, enabling evaluation of the insulated and uninsulated structures in various solvents. Insulation of the coumarin fluorophore demonstrated blue-shifted absorption and emission wavelengths in almost all the solvents, similar to those seen in MeCN. Moreover, the absorption and emission wavelengths of *ins-CM* and *uns-CM* increased with increasing solvent polarities, which is attributable to their ICT states, where higher solvent polarity results in greater solvent relaxation in the excited state.¹⁶ The Stokes shifts of *ins-CM* and *uns-CM* increased comparably with increasing polarities of the solvents according to the Lippert-Mataga expression, indicating that they form identical ICT states in their excited states in all solvents (Fig. S3).

The insulation effects on the fluorescent quantum yield showed a clear polarity-dependent trend when each solvent was classified as having low (benzene, toluene), medium (CHCl₃, EtOAc, THF, CH₂Cl₂, CH₄Cl₂), or high polarity (DMSO, *i*PrOH, acetone, EtOH, MeCN, MeOH) in the solvent polarity function (Δf).¹⁷ In the case of low-polarity solvents, the insulated coumarin had a high quantum yield of ~80%, which was slightly lower than that of uninsulated coumarin (~90%) in the same solvents (Fig. 3b, yellow region). The relatively low quantum yields of insulated coumarin in low-polarity solvents may be attributed to the supramolecular interaction between the coumarin moiety and PM α -CD; the quantum yield could be equivalent to that of coumarin wrapped with methylated glucopyranose moieties. In contrast, in the case of medium-polarity solvents, the quantum yields of *uns-CM* drastically decreased, whereas those of *ins-CM* remained almost

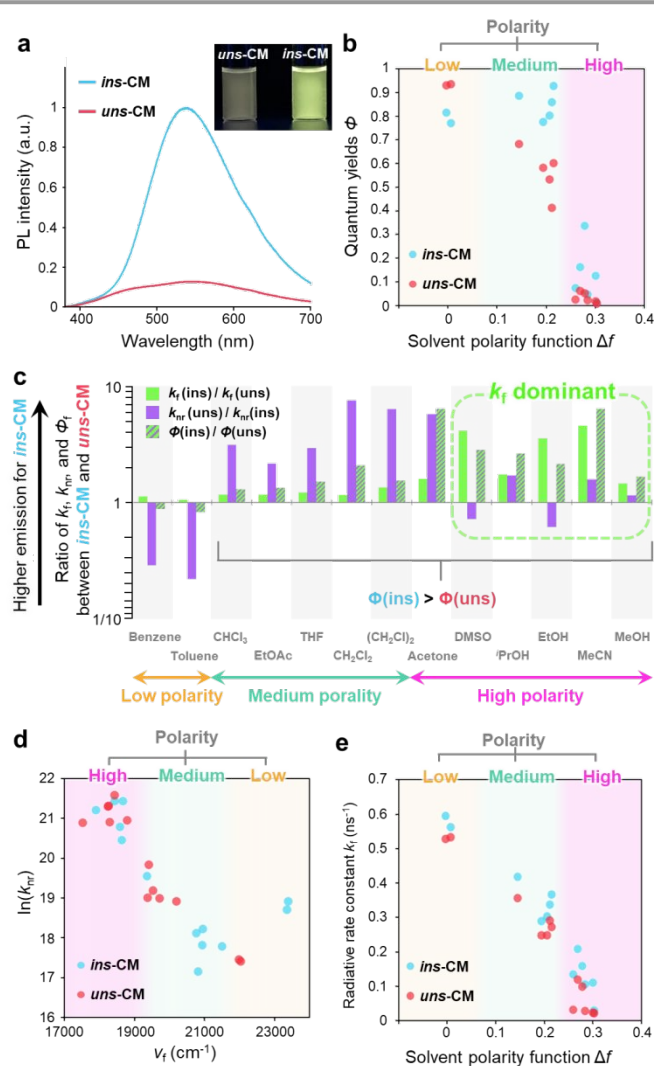


Fig. 3. (a) Emission spectra and photographs of *ins-CM* and *uns-CM* in MeCN at the excitation wavelength (365 nm). Emission spectra were normalized to an equal number of absorbed photons. (b) Quantum yield of *ins-CM* and *uns-CM* as a function of the solvent polarity (Δf). (c) Logarithmic bar graph of $k_f(\text{ins-CM})/k_f(\text{uns-CM})$, $k_{nr}(\text{uns-CM})/k_{nr}(\text{ins-CM})$, and $\Phi(\text{ins-CM})/\Phi(\text{uns-CM})$ calculated for each solvent. (d) Correlation between the natural logarithm of the nonradiative rate constant and the emission maxima. (e) Correlation between the radiative rate constant and the solvent polarity function.

unchanged (Fig. 3b, green region), indicating that the insulated coumarin exhibited a higher quantum yield than the uninsulated coumarin (Fig. 3c). In the medium-polarity solvent region, the proportional relationship between the natural logarithm of the nonradiative decay rate constant ($\ln(k_{nr})$) and emission maxima ($\nu_f \text{ cm}^{-1}$) satisfied the energy gap law¹⁸ for both *ins*-CM and *uns*-CM (Fig. 3d, green region). Hence, the enhancement of the quantum yield in these solvents could be attributed to a smaller nonradiative decay rate constant (k_{nr}) of the insulated coumarin than that of the uninsulated coumarin. The smaller k_{nr} in *ins*-CM may be attributed to a larger S_0 - S_1 energy gap and smaller Frank-Condon factor owing to the shorter effective conjugation length of its π -conjugated system.

Furthermore, *ins*-CM exhibited higher quantum yields than *uns*-CM even in the high-polarity solvent group (Fig. 3b, pink). In these solvents, the fluorescence rate constant (k_f) was increased by insulation, as represented by *ins*-CM in MeCN (Table 1). To determine the primary kinetic factor for enhancing the quantum yield through insulation, the insulation effects on the nonradiative decay rate constant (k_{nr}) and fluorescence rate constant (k_f) were evaluated by comparing the ratios of $k_f(\textit{ins}\text{-CM})/k_f(\textit{uns}\text{-CM})$ and $k_{nr}(\textit{uns}\text{-CM})/k_{nr}(\textit{ins}\text{-CM})$ in each solvent (Fig. 3c), where larger values indicated higher emission in *ins*-CM. Consequently, the higher fluorescent quantum yields achieved through insulation were predominantly attributed to k_{nr} in medium-polarity solvents and to k_f in high-polarity solvents. Indeed, a negative relationship was observed between k_f and Δf , even in the case of *ins*-CM, but the k_f of *ins*-CM was higher than that of *uns*-CM in all solvents, indicating the effectiveness of insulation for enhancing quantum yields (Fig. 3e). Here, the decrease in k_f in high-polarity solvents was caused by solvent-induced structural changes that occurred to stabilize the excited dipole states of *ins*-CM and *uns*-CM.¹⁹ Thus, the significantly improved quantum yield and the increase in the k_f of *ins*-CM could be attributed to the conformational locking of coumarin with PM α -CD, which prevents the polarity-induced orthogonalization of the two phenylene rings.²⁰

3. Conclusions

In summary, the luminescence properties of a coumarin-[1]rotaxane structure were systematically investigated in solvents of various polarities. Insulation improved the fluorescent quantum yields, especially in medium- and high-polarity solvents. The k_{nr} of the [1]rotaxane structure decreased owing to the twisting of the π -conjugated system, whereas k_f increased because the polarity-induced structural change of the molecule was effectively suppressed by the insulation. These results could inspire new luminescent chromophore designs of [1]rotaxane structures to improve luminescent quantum yields by controlling solvation-induced effects in the excited-state dynamics. These high-performance luminescent materials have potential applications as bioprobes in aqueous solutions.²¹

4. Experimental

4.1. Materials

All reagents were commercially obtained and used as received unless otherwise noted. The compound **1**¹¹ and 7-iodo-4-methylcoumarin²² were prepared according to the reported procedures. THF was purchased from Kanto Chemical and further purified by passage through activated alumina under positive nitrogen pressure as described by Grubbs et al.²³

4.2. Instruments

NMR Spectroscopy. ¹H NMR (500 MHz), ROESY NMR (500 MHz), and ¹³C{¹H} NMR (126 MHz) were measured with a Bruker AVANCE III HD 500 spectrometer. The ¹H NMR chemical shifts were reported relative to tetramethylsilane (TMS, 0.00 ppm) or residual protonated solvents (7.26 ppm) in CDCl₃. The ¹³C{¹H} NMR chemical shifts were reported relative to ¹³CDCl₃ (77.16 ppm). ¹H DOSY NMR were measured with a Bruker AVANCE HD 500 spectrometer.

High-Resolution Mass Spectroscopy (HR-MS). Electrospray ionization time-of-flight (ESI-TOF) mass spectra were recorded on micrOTOF II-KE02 using internal mass calibration with NaTFA or CsI cluster ions.

Preparative Recycling Gel Permeation Chromatography (GPC). Preparative recycling GPC was performed with a Shimadzu LC-20AP System equipped with Shodex K-4002L and Shodex K-4002.5L columns, a Shimadzu SPD-20A, and a Shimadzu RID-10A, or a JAI LC9130NEXT System equipped with JAIGEL-2H and 2.5H columns, a JAI UV DETECTOR 370NEXT, and a JAI RI DETECTOR RI 700NEXT using CHCl₃ as the eluent at a flow rate of 14 ml min⁻¹.

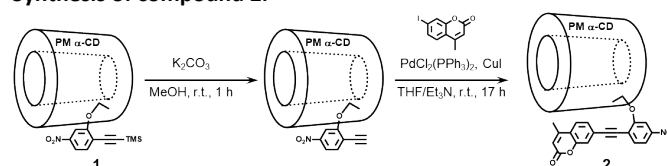
Absorption Spectroscopy. Ultraviolet-visible absorption spectra were measured at a concentration of 1.0×10^{-5} M with a Shimadzu UV-2600 model.

Luminescence Spectroscopy and Quantum Yield Measurements. Emission spectra were measured with a Shimadzu RF-6000 Spectro Fluorophotometer. Emission spectra and absolute quantum yields were measured at a concentration of 1.0×10^{-5} M with an absolute PL quantum yield spectrometer (Quantaaurus-QY, C11347, Hamamatsu Photonics) bearing a calibrated integrating sphere system. This system consists of an excitation light source, a sample holder mounted in an integrating sphere and a multi-channel CCD spectrometer.

Luminescence Lifetime Measurements. Luminescence lifetimes were measured at a concentration of 1.0×10^{-5} M with a lifetime measurement system (Quantaaurus-Tau, C11367G, Hamamatsu Photonics) based on the time-correlated single photon counting (TCSPC). The lifetime was obtained by fitting to the monoexponential or biexponential decay functions.

4.3. Synthetic procedures

Synthesis of compound 2.



1 (300.2 mg, 0.210 mmol) and K_2CO_3 (87.4 mg, 0.632 mmol) were dissolved in MeOH (6.1 ml) under a nitrogen atmosphere. The reaction mixture was stirred at room temperature. After 1 h stirring, the mixture was dried *in vacuo* and then filtered through a Celite pad eluting with $CHCl_3$. The obtained solution was concentrated, and the crude product was used immediately without further purification. To the crude product were added THF (13 ml) and Et_3N (0.43 ml) and then stirred under nitrogen bubbling for 10 min. Under a nitrogen atmosphere, 7-iodo-4-methylcoumarin (50.0 mg, 0.175 mmol), CuI (1.1 mg, 5.8 μ mol), and $PdCl_2(PPh_3)_2$ (7.2 mg, 10 μ mol) were added into the solution, and then the reaction mixture was stirred at room temperature for 16 h. The reaction mixture was then washed with NH_4Cl (aq.) solution. The aqueous layer was extracted with CH_2Cl_2 . The combined organic layers were dried using Na_2SO_4 , filtered, and concentrated *in vacuo*. The residue was further purified by GPC with $CHCl_3$ as the eluent to yield **2** as a yellow solid (194.0 mg, 73%).

ESI HR-MS: (m/z) 1536.6283 ($[M+Na]^+$, $C_{71}H_{103}NO_{34}Na$, calcd. 1536.6254).

1H NMR (500 MHz, $CDCl_3$, r.t.): $\delta_H = 7.86$ (d, $J = 8.4$ Hz, 1H, ArH), 7.81 (s, 1H, ArH), 7.65 (d, $J = 8.4$ Hz, 1H, ArH), 7.60 (s, 1H, ArH), 7.58 (d, $J = 8.4$ Hz, 1H, ArH), 7.53 (d, $J = 8.2$ Hz, 1H, ArH), 6.33 (s, 1H, C=C(H)-CO), 5.11-3.02 (m, 93H, CD-H, OCH_3), 2.46 (s, 3H, CH_3).

^{13}C NMR (126 MHz, $CDCl_3$, r.t.): $\delta_C = 160.19, 159.78, 153.54, 151.54, 148.47, 133.66, 127.65, 125.93, 124.78, 120.64, 120.18, 119.31, 116.11, 116.08, 107.00, 100.59, 100.45, 100.37, 100.32, 100.27, 100.24, 96.90, 87.52, 82.88, 82.74, 82.68$ (several peaks overlapped), 82.64, 82.38, 82.34, 82.31 (several peaks overlapped), 82.19, 82.11, 81.34 (several peaks overlapped), 81.32 (several peaks overlapped), 81.24, 81.15, 71.86 (several peaks overlapped), 71.69, 71.67, 71.65, 71.62, 71.48, 71.45, 71.42, 71.35, 70.36, 68.56, 61.98 (several peaks overlapped), 61.96 (several peaks overlapped), 61.93 (several peaks overlapped), 59.46, 59.25 (several peaks overlapped), 59.03, 58.39, 58.06, 58.01, 57.96, 57.94, 57.58, 18.74.

Synthesis of *uns-CM*. 2 (194.0 mg, 0.128 mmol) was added to a mixture of EtOH (7.3 ml) and THF (7.3 ml) followed by nitrogen bubbling for 10 min. Into the solution, Zn (415.1 mg, 6.38 mmol) and NH_4Cl (472.3 mg, 8.43 mmol) were added, and the solution was vigorously stirred at room temperature for 1 h. The mixture was filtered through a Celite pad and then washed with CH_2Cl_2 and H_2O . The aqueous layer was extracted with CH_2Cl_2 and Et_2O . The combined organic layers were dried using Na_2SO_4 , filtered, and concentrated *in vacuo*. The residue was further purified by GPC with $CHCl_3$ as the eluent to yield ***uns-CM*** as a yellow solid (113.2 mg, 60%).

ESI HR-MS: (m/z) 1506.6533 ($[M+Na]^+$, $C_{71}H_{105}NO_{32}Na$, calcd. 1506.6512).

1H NMR (500 MHz, $CDCl_3$, r.t.): $\delta_H = 7.51$ -7.50 (m, 2H, ArH), 7.45 (d, $J = 8.2$ Hz, 1H, ArH), 7.29-7.26 (peak overlapped with $CHCl_3$, 1H, ArH), 6.27-6.26 (m, 2H, ArH), 6.22 (s, 1H, C=C(H)-CO), 5.15-3.08 (m, 95H, CD-H, OCH_3 , NH_2), 2.43 (s, 3H, CH_3).

^{13}C NMR (126 MHz, $CDCl_3$, r.t.): $\delta_C = 161.00, 160.73, 153.52, 151.91, 149.08, 134.66, 128.18, 127.18, 124.35, 119.19, 119.11,$

114.94, 107.69, 102.08, 100.48, 100.39, 100.30, 100.20, 100.17, 99.81, 99.35, 91.20, 90.73, 82.91, 82.69, 82.62 (several peaks overlapped), 82.46, 82.43, 82.31 (several peaks overlapped), 82.29 (several peaks overlapped), 82.22, 82.12, 81.33, 81.30 (several peaks overlapped), 81.27, 81.25, 81.21, 71.92, 71.67, 71.62, 71.56, 71.52, 71.49 (several peaks overlapped), 71.40, 71.39, 71.36, 70.46, 67.96, 61.98, 61.91 (several peaks overlapped), 61.87, 61.83, 59.28, 59.17 (several peaks overlapped), 59.11, 59.02, 58.31, 58.04, 58.02, 57.95, 57.92, 57.57, 18.70.

Synthesis of *ins-CM*. *uns-CM* (33.7 mg, 0.022 mmol) was dissolved in MeOH (10 ml) and H_2O (10 ml). Under a nitrogen atmosphere, the mixture was stirred at room temperature overnight. The mixture was dried *in vacuo*, and the residue was diluted with water. The organic layer was extracted with $CHCl_3$ and Et_2O , and then dried with Na_2SO_4 . The solvent was removed *in vacuo* to yield ***ins-CM*** as a yellow solid (33.0 mg, 98%).

ESI HR-MS: (m/z) 1506.6524 ($[M+Na]^+$, $C_{71}H_{105}NO_{32}Na$, calcd. 1506.6512).

1H NMR (500 MHz, $CDCl_3$, r.t.): $\delta_H = 8.00$ (d, $J = 1.1$ Hz, 1H, ArH), 7.96 (dd, $J = 8.2$ Hz, $J = 1.4$ Hz, 1H, ArH), 7.70 (d, $J = 8.2$ Hz, 1H, ArH), 7.27-7.26 (peak overlapped with $CHCl_3$, 1H, ArH), 6.46-6.44 (m, 2H, ArH), 6.21 (s, 1H, C=C(H)-CO), 5.10-2.85 (m, 95H, CD-H, OCH_3 , NH_2), 2.32 (s, 3H, CH_3).

^{13}C NMR (126 MHz, $CDCl_3$, r.t.): $\delta_C = 163.82, 159.50, 153.62, 150.63, 149.39, 134.43, 128.52, 126.94, 124.10, 119.63, 119.52, 115.64, 109.98, 108.02, 104.90, 100.93, 100.55, 100.35, 100.10$ (several peaks overlapped), 98.34, 91.71, 90.49, 84.07, 82.93, 82.70, 82.50 (several peaks overlapped), 82.44, 82.36, 82.26, 82.22, 82.12, 82.08, 81.73, 81.61, 81.51, 81.49, 81.36 (several peaks overlapped), 81.27, 76.11, 72.48, 72.04, 71.91, 71.52 (several peaks overlapped), 71.39, 71.25 (several peaks overlapped), 70.77, 70.26, 62.05 (several peaks overlapped), 61.89, 61.82, 61.57, 61.47, 59.21, 59.19, 59.03, 58.86, 58.83, 58.39, 58.28, 58.00, 57.86 (several peaks overlapped), 57.76, 18.27.

Conflicts of interest

There are no conflicts to declare.

Acknowledgements

This research was supported by financial supports (JSPS KAKENHI Grant Numbers 18H05158, 19H02696, 19K22179, and 19K15629, JST CREST Grant Number JPMJCR1912, and JST PRESTO Grant Number JPMJPR21N8).

Notes and references

- (a) M. Lu, Y. Zhang, S. Wang, J. Guo, W. W. Yu and A. L. Rogach, *Adv. Funct. Mater.*, 2019, **29**, 1902008.; (b) L. Feng, C. Zhu, H. Yuan, L. Liu, F. Lv and S. Wang, *Chem. Soc. Rev.*, 2013, **42**, 6620; (c) G. Xu, S. Zeng, B. Zhang, M. T. Swihart, K. T. Yong and P. N. Prasad, *Chem. Rev.*, 2016, **116**, 12234.

- 2 (a) A. D. Nidhankar, Goudappagouda, V. C. Wakchaure and S. S. Babu, *Chem. Sci.*, 2021, **12**, 4216; (b) H. Lu, J. MacK, Y. Yang and Z. Shen, *Chem. Soc. Rev.*, 2014, **43**, 4778.
- 3 (a) B. Shi, K. Jie, Y. Zhou, J. Zhou, D. Xia and F. Huang, *J. Am. Chem. Soc.*, 2016, **138**, 80; (b) W. C. Wu, C. Y. Chen, Y. Tian, S. H. Jang, Y. Hong, Y. Liu, R. Hu, B. Z. Tang, Y. T. Lee, C. T. Chen, W. C. Chen and A. K. Y. Jen, *Adv. Funct. Mater.*, 2010, **20**, 1413; (c) S. Tao, S. Zhu, T. Feng, C. Zheng and B. Yang, *Angew. Chem. Int. Ed.*, 2020, **59**, 9826. (d) D. Li, F. Lu, J. Wang, W. Hu, X.-M. Cao, X. Ma, H. Tian, *J. Am. Chem. Soc.*, 2018, **140**, 1916.
- 4 (a) M. Frampton and H. Anderson, *Angew. Chem. Int. Ed.*, 2007, **46**, 1028; (b) H. Masai, Y. Oka and J. Terao, *Chem. Commun.*, 2022, **58**, 1644; (c) C. Pan, C. Zhao, M. Takeuchi and K. Sugiyasu, *Chem. Asian J.*, 2015, **10**, 1820.
- 5 (a) S. Anderson and H. L. Anderson, *Angew. Chem. Int. Ed. Engl.*, 1996, **35**, 1956; (b) P. Hazra, D. Chakrabarty, A. Chakraborty and N. Sarkar, *Chem. Phys. Lett.*, 2004, **388**, 150; (c) X. K. Ma, W. Zhang, Z. Liu, H. Zhang, B. Zhang and Y. Liu, *Adv. Mater.*, 2021, **33**, 2007476.
- 6 J. R. Lakowicz, in *Effects of Solvents on Fluorescence Emission*, Springer, US, Boston, MA, 1983, pp. 187–215.
- 7 S. S. Andersen, A. W. Saad, R. Kristensen, T. S. Pedersen, L. J. O'Driscoll, A. H. Flood and J. O. Jeppesen, *Org. Biomol. Chem.*, 2019, **17**, 2432.
- 8 A. Martinez-Cuezva, F. Morales, G. R. Marley, A. Lopez-Lopez, J. C. Martinez-Costa, D. Bautista, M. Alajarin and J. Berna, *European J. Org. Chem.*, 2019, **2019**, 3480.
- 9 C. A. Stanier, S. J. Alderman, T. D. W. Claridge and H. L. Anderson, *Angew. Chem. Int. Ed.*, 2002, **41**, 1769.
- 10 H. Masai, T. Fujihara, Y. Tsuji and J. Terao, *Chem. Eur. J.*, 2017, **23**, 15073.
- 11 H. Masai, J. Terao, T. Fujihara and Y. Tsuji, *Chem. Eur. J.*, 2016, **22**, 6624.
- 12 (a) H. Masai, J. Terao, S. Makuta, Y. Tachibana, T. Fujihara and Y. Tsuji, *J. Am. Chem. Soc.*, 2014, **136**, 14714; (b) G. M. Russell, D. Inamori, H. Masai, T. Tamaki and J. Terao, *Polym. Chem.*, 2019, **10**, 5280; (c) T. Hosomi, H. Masai, T. Fujihara, Y. Tsuji and J. Terao, *Angew. Chem. Int. Ed.*, 2016, **55**, 13427; (d) H. V. Miyagishi, H. Masai and J. Terao, *Chem. Eur. J.*, 2022, **28**, e202103175; (e) S. Shimada, H. V. Miyagishi, H. Masai, Y. Masui and J. Terao, *Bull. Chem. Soc. Jpn.*, 2021, 163.
- 13 B. D. Wagner, *Molecules*, 2009, **14**, 210.
- 14 R. Nishiyabu and K. Kano, *European J. Org. Chem.*, 2004, 4988.
- 15 T. Fujimoto, Y. Sakata and T. Kaneda, *Chem. Commun.*, 2000, 2143.
- 16 S. C. A. Yeh, M. S. Patterson, J. E. Hayward and Q. Fang, *Photonics*, 2014, **1**, 530.
- 17 Δf is defined by the following equation: $\Delta f = (\epsilon - 1)/(2\epsilon + 1) - (n^2 - 1)/(2n^2 - 1)$ where ϵ and n are the dielectric constant and refractive index of the solvents, respectively.
- 18 G. E. Shillito, T. B. J. Hall, D. Preston, P. Traber, L. Wu, K. E. A. Reynolds, R. Horvath, X. Z. Sun, N. T. Lucas, J. D. Crowley, M. W. George, S. Kupfer and K. C. Gordon, *J. Am. Chem. Soc.*, 2018, **140**, 4534.
- 19 A. C. Benniston, A. Harriman and J. P. Rostron, *Phys. Chem. Chem. Phys.*, 2005, **7**, 3041.
- 20 The polarity-induced decrease in k_f of **uns-CM** is attributable to the orthogonalization of two phenylene moieties in **uns-CM** because a rigid coumarin derivative (e.g. 7-amino-4-methylcoumarin) shows less decrease in k_f values compared with **uns-CM**. See: H. Pal, S. Nad and M. Kumbhakar, *J. Chem. Phys.*, 2003, **119**, 443.
- 21 S. Biswas, Y. Rajesh, S. Barman, M. Bera, A. Paul, M. Mandal and N. D. Pradeep Singh, *Chem. Commun.*, 2018, **54**, 7940.
- 22 T. N. Pahattuge, J. M. Jackson, R. Digamber, H. Wijerathne, V. Brown, M. A. Witek, C. Perera, R. S. Givens, B. R. Peterson and S. A. Soper, *Chem. Commun.*, 2020, **56**, 4098.
- 23 A. B. Pangborn, M. A. Giardello, R. H. Grubbs, R. K. Rosen and F. J. Timmer, *Organometallics*, 1996, **15**, 5, 1518.